AGU PUBLICATIONS

JGR

Journal of Geophysical Research: Oceans

RESEARCH ARTICLE

10.1002/2017JC013067

Key Points:
- Calibration of physical and optical data from the SOCLIM cruise in terms of plankton assemblage in the Southern Ocean (SO)
- Prediction of plankton groups from biogeochemical Argo floats data in the vicinity of the calibration area (Indian sector of the SO)
- Spatial and seasonal changes in plankton assemblage described at high resolution and compared with large particle export in the mesopelagic

Supporting Information:
- Supporting Information S1
- Data Set S1

Correspondence to:
M. Rembauville,
mathieurembauville@gmail.com

Citation:
Rembauville, M., Briggs, N., Ardyna, M., Uitz, J., Catala, P., Penkerc'h, C., . . . Blain, S. (2017). Plankton assemblage estimated with BGC-Argo floats in the Southern Ocean: Implications for seasonal successions and particle export. *Journal of Geophysical Research: Oceans*, *122*, 8278–8292. https://doi.org/10.1002/2017JC013067

Received 11 MAY 2016
Accepted 23 SEP 2017
Accepted article online 27 SEP 2017
Published online 30 OCT 2017

Plankton Assemblage Estimated with BGC-Argo Floats in the Southern Ocean: Implications for Seasonal Successions and Particle Export

Mathieu Rembauville[1], Nathan Briggs[1], Mathieu Ardyna[1], Julia Uitz[1], Philippe Catala[2], Cristophe Penkerc'h[1], Antoine Poteau[1], Hervé Claustre[1], and Stéphane Blain[2]

[1]Sorbonne Universités, UPMC Univ Paris 06, INSU-CNRS, Laboratoire d'Océanographie de Villefranche, Villefranche-sur-mer, France, [2]Sorbonne Universités, UPMC Univ Paris 06, CNRS, Laboratoire d'Océanographie Microbienne (LOMIC), Observatoire Océanologique, Banyuls/mer, France

Abstract The Southern Ocean (SO) hosts plankton communities that impact the biogeochemical cycles of the global ocean. However, weather conditions in the SO restrict mainly *in situ* observations of plankton communities to spring and summer, preventing the description of biological successions at an annual scale. Here, we use shipboard observations collected in the Indian sector of the SO to develop a multivariate relationship between physical and bio-optical data, and, the composition and carbon content of the plankton community. Then we apply this multivariate relationship to five biogeochemical Argo (BGC-Argo) floats deployed within the same bio-geographical zone as the ship-board observations to describe spatial and seasonal changes in plankton assemblage. The floats reveal a high contribution of bacteria below the mixed layer, an overall low abundance of picoplankton and a seasonal succession from nano- to microplankton during the spring bloom. Both naturally iron-fertilized waters downstream of the Crozet and Kerguelen Plateaus show elevated phytoplankton biomass in spring and summer but they differ by a nano- or microplankton dominance at Crozet and Kerguelen, respectively. The estimated plankton group successions appear consistent with independent estimations of particle diameter based on the optical signals. Furthermore, the comparison of the plankton community composition in the surface layer with the presence of large mesopelagic particles diagnosed by spikes of optical signals provides insight into the nature and temporal changes of ecological vectors that drive particle export. This study emphasizes the power of BGC-Argo floats for investigating important biogeochemical processes at high temporal and spatial resolution.

1. Introduction

The Southern Ocean (SO) plays a key role in the global carbon cycle representing 40% of the oceanic anthropogenic CO_2 sink (Mikaloff Fletcher et al., 2006; Sabine et al., 2004). The SO displays highly contrasted surface chlorophyll *a* concentrations and associated primary production (Ardyna et al., 2017; Arrigo et al., 2008). The vast high nutrient, low chlorophyll (HNLC, Minas et al., 1986) areas characterized by iron limitation (de Baar et al., 1990; Martin et al., 1990) contrast with highly productive areas supported by natural iron fertilization (Boyd et al., 2012). Additionally, the strong eastward-flowing Antarctic Circumpolar Current generates stable fronts, imposing a hydrological zonation that constrains phytoplankton species distribution (Charalampopoulou et al., 2016; Crosta et al., 2005; Diíez et al., 2004). Sampling this biological diversity is a critical step for a better understanding of how plankton assemblage shapes biogeochemical fluxes such as the carbon transfer to the ocean interior (Boyd & Newton, 1999; Guidi et al., 2015; Henson et al., 2012). For example, it is suggested that microplankton-dominated communities show high export efficiency but low transfer efficiency, whereas the opposite is observed for picoplankton (Guidi et al., 2015; Henson et al., 2012).

The weather conditions in the SO restrict *in situ* observations with classical oceanographic cruises mainly in spring and summer. To overcome this issue, phytoplankton seasonal dynamics have been studied using satellite ocean color data coupled with climatologies of physical data (Ardyna et al., 2017; Fauchereau et al., 2011; Thomalla et al., 2011). However, these approaches are limited to the upper layer of the ocean and might miss important features of phytoplankton vertical distribution (Erickson et al., 2016; Holm-Hansen &

Hewes, 2004; Parslow et al., 2001). In addition, the observations of ocean colour in the SO in winter are impaired by the presence of sea-ice and persistent cloud cover (Pope et al., 2017). The recent development of autonomous observation platforms equipped with bio-optical sensors such as gliders and especially the so-called Biogeochemical-Argo (BGC-Argo) floats (Johnson & Claustre, 2016) offers the opportunity to study phytoplankton geographical, vertical and temporal distribution in the critically under-sampled SO waters.

Concomitantly, recent methods have been developed to estimate biogeochemical fluxes from autonomous observations such as primary production (Nicholson et al., 2015; Thomalla et al., 2015), export (Bishop et al., 2004; Briggs et al., 2011; Estapa et al., 2017) and remineralization (Hennon et al., 2016; Martz et al., 2008). However, the identification of the biological drivers of these fluxes is generally elusive because the interpretation of the bio-optical signals in terms of particle assemblages remains complex. For example, according to theory, particulate backscattering coefficient (b_{bp}) is mostly influenced by $\sim$1 μm sized particles, but field studies have shown that plankton of much larger size can potentially affect b_{bp} (Morel & Ahn, 1991; Stramski & Kiefer, 1991). Moreover, laboratory studies with monospecific cultures have demonstrated that for a given cell size, both cell structure and shape affects the b_{bp} signal (Vaillancourt et al., 2004; Volten et al., 1998; Whitmire et al., 2010). Similarly, variations in the chlorophyll *a* fluorescence to particulate backscattering ratio can reflect both photoacclimation processes (Behrenfeld & Boss, 2003) and changes in the phytoplankton community structure (Cetinić et al., 2015). Thus, the bio-optical signals collected by autonomous platforms result from a complex combination of multiple factors (plankton community structure, phytoplankton physiology, abiotic particles). In this context, the characterization of the co-variation of optical signals and plankton community structure in a given environment is clearly needed before unambiguously interpreting the data reported by autonomous platforms.

The SOCLIM (Southern Ocean and CLIMate) project aims to study climate-relevant biogeochemical processes in the Southern Ocean by combining classical oceanographic sampling with innovative tools (e.g., BGC-Argo floats, moored autonomous water samplers). In this study, we first aim at developing a multivariate transfer function that allows, based on data acquired during the SOCLIM cruise (October 2016), relationships to be established between hydrological and optical signals and the plankton community structure from bacteria to microplankton. This transfer function is subsequently applied to data collected by five BGC-Argo floats deployed in the Indian sector of the SO to predict and analyze the variability of plankton community structure for diverse seasons and environments of the SO. Finally, we detail the relationship between the predicted plankton community structure in the mixed layer and the occurrence of large particles in the mesopelagic.

2. Methods

2.1. Plankton Carbon Estimation and Optical Data Collected During the SOCLIM Cruise

The SOCLIM cruise (DOI:10.17600/16003300) took place in the Indian sector of the SO in October 2016 on board the R/V *Marion Dufresne II*. Conductivity-temperature-depth (CTD, Seabird SBE9+) casts were performed at various stations from the Subtropical Zone to the Antarctic Zone. We focus here on 11 stations located between 35°S and 58.5°S (Figure 1a and supporting information Table S1). Vertical profiles of chlorophyll *a* fluorescence (F), particulate backscattering at 700 nm (b_{bp}) and particulate beam attenuation coefficient at 650 nm (c_p) were acquired using a Wet Labs ECO triplet and a Wet Labs C-star transmissiometer (25 cm path length) mounted on the CTD frame. Fluorescence data were corrected for non-photochemical quenching on daytime profiles following the method of Xing et al. (2012) and converted to chlorophyll *a* concentration (Chl, mg m^{-3}) by first applying the factory calibration (dark value and slope) and then multiplying by 0.5 (Roesler et al., 2017). b_{bp} (m^{-1}) was calculated as described in Schmechtig et al. (2015) and references therein. Briefly, raw instrument measurements (counts) were transformed into the total volume scattering function (β) at an angle of 124° and wavelength of 700 nm by applying the manufacturer-provided scaling factor and dark count. b_{bp} was then calculated as $b_{bp}=2\pi\chi(\beta-\beta_{sw})$ where χ is a wavelength-dependent conversion factor (here 1.142) and β_{sw} is the contribution of pure seawater to scattering that depends on temperature and salinity. c_p (m^{-1}) was calculated from transmittance data (T) using the manufacturer calibration: $c_p=-\frac{1}{l}\times\ln(T)$ where l is the sensor pathlenth (25 cm) and $T=\frac{V_s-V_d}{V_w-V_d}$ where V_s in the instrument signal, V_d is the dark value and V_w is the value in the water used for calibration. The windows of the optical instruments were carefully cleaned before each deployment and no drift correction was

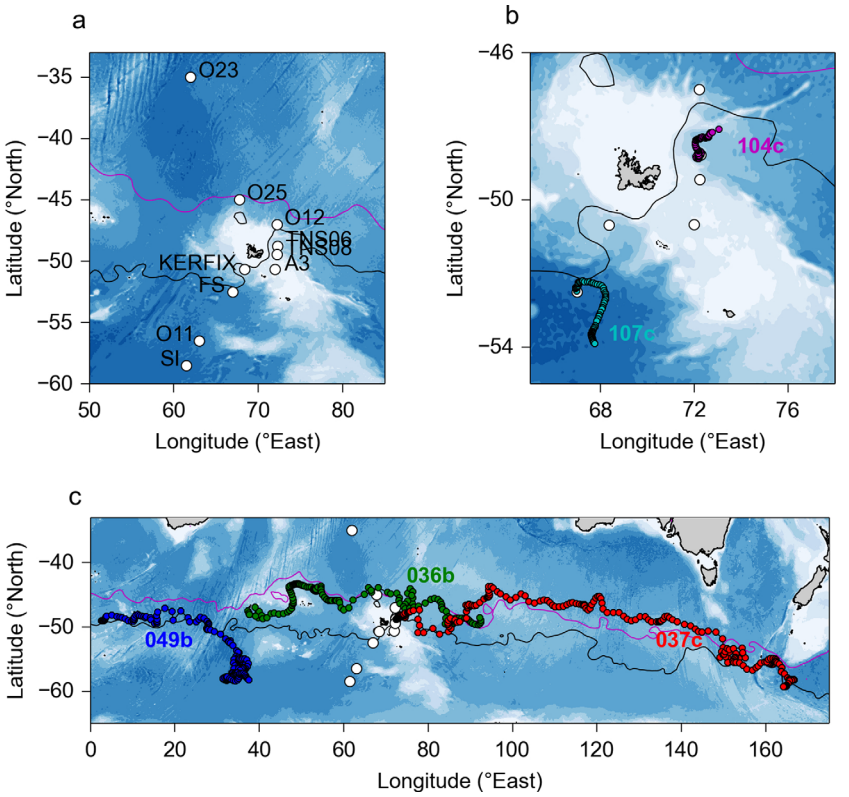

Figure 1. (a) Location of the SOCLIM cruise stations (white dots) where data have been used to train the PLSR between optical signals and the plankton community composition. (b and c) Trajectories of five BGC-Argo floats in the Indian sector of Southern Ocean used to test the PLSR and predict plankton assemblage from float optical data. Magenta and black lines represent respectively the climatological location of the Subantarctic and Polar Front derived from satellite-derived altimetry (Swart et al., 2010).

applied to the ship data (see section 2.2). Spikes were removed from the Chl and b_{bp} signals by applying a low-pass filter that consists of a 5-point running median followed by a 7-point running mean (Briggs et al., 2011). Finally the CTD and optical data were averaged at the depth corresponding to the sampling for plankton diversity (± 1 m).

Samples for plankton community composition were acquired at 3 different depths (250 m, 100 m and surface between 5 and 10 m depending on the swell). For flow cytometry analyses, 9 mL of seawater were

Table 1
Plankton Groups Considered in This Study and Their Associated Characteristics

Plankton group	Contains	Method	Volume (μm^3)	Carbon content (pgC)
Bact	Heterotrophic bacteria	Cytometry	0.25[a]	0.015[a]
Pico	Prochlorococcus		0.68[b]	0.029[b]
	Synechococcus		0.86[b]	0.080[b]
	Picoeukaryotes		2.76[b]	0.73[b]
Nano	Nanoplankton		284[c]	15[c]
Micro	Diatom (55 groups)	Optical microscopy	Shape-specific	$C=0.117V^{0.881}$[d]
	Dinoflagellate (14 groups)		Shape-specific	$C=0.760V^{0.819}$[d]
	Ciliate (4 groups)		Shape-specific	$C=0.216V^{0.939}$[d]
	Silicoflagellate (1 group)		3288	$C=0.261V^{0.860}$[d]

[a]Bratbak (1985).
[b]Grob et al. (2007).
[c]Verity et al. (1992).
[d]Menden-Deuer and Lessard (2000).

Table 2
Results From the Bootstrapping Technique Used to Estimate the Quality of Prediction of the PLSR. Coefficient of Determination (R^2) and Root Mean Square Error (RMSE) of the Observed Versus Predicted $\%C_{group}$ for Each Plankton Group and for the Pooled Plankton Groups

Plankton group	R^2	RMSE (%)
Bact	0.71 ± 0.11	14 ± 4
Pico	0.61 ± 0.15	26 ± 12
Nano	0.65 ± 0.13	19 ± 6
Micro	0.59 ± 0.14	17 ± 5
Global	0.84 ± 0.06	6 ± 1

Note: The mean ± standard deviation resulting from 10,000 calculations is given.

sampled from the Niskin bottles, fixed with glutaraldehyde (0.5% final concentration), flash-frozen in liquid nitrogen, and stored at −80°C. The abundance of heterotrophic bacteria (including Bacteria and Archaea), pico- and nanoplankton was measured by flow cytometry using a FACSCalibur instrument (Marie et al., 2001). Bacteria, pico- and nanoplankton biovolume and carbon content were estimated using constant cell volume and cell carbon content from the literature (Table 1).

For microplankton abundance and diversity, 100 mL of seawater was sampled in opaque bottles, fixed with acidic lugol (1% final concentration) and stored at 4°C. Back in the laboratory, samples were sedimented into an Utermöhl counting chamber (24 h, dark). Microplankton cells were enumerated and identified to the lowest taxonomic level using an inverted microscope with phase contrast (Olympus IX70) at X400 magnification. 500 to 1,500 cells per sample were enumerated and species were identified following recommendations by Hasle and Syvertsen (1997). Samples were counted within 2 months following the sampling. Morphometric measurements were made from high-resolution images (Olympus DP71 camera) using the Fiji image processing package (available at http://fiji.sc/Fiji). Biovolume of each microplankton species/group was estimated from morphometric measurements (performed on 20 individuals randomly selected for each species/group) and shape-specific equations (Hillebrand et al., 1999). Carbon content of each microplankton group was calculated using group-specific equations from the literature (Table 1). The full list of microplankton groups/species and the associated biovolume is given in the supporting information data set. The total plankton carbon (C_{tot}) was defined as the sum of bacteria, pico-, nano- and microplankton carbon biomass: $C_{tot} = C_{Bact} + C_{Pico} + C_{Nano} + C_{Micro}$. The relative contribution of each group to C_{tot} was calculated as $\%C_{group} = C_{group}/C_{tot}$. The definition of each plankton group and the associated carbon content are given in Table 1.

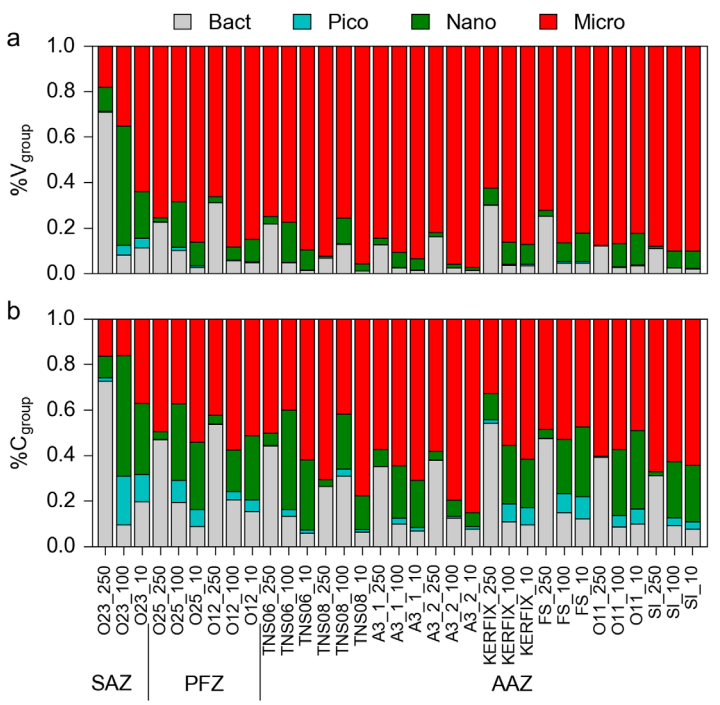

Figure 2. Relative contribution of each plankton class to (a) the total plankton volume and (b) the total plankton carbon for each samples from the SOCLIM cruise. Sample labels refer to the station and the sampling depth (from left to right: 250 m, 100 m and 10 m for each station), SAZ: Subantarctic Zone, PFZ: Polar Frontal Zone, AAZ: Antarctic zone.

For particulate organic carbon (POC) analysis, 2 L of seawater were sampled at 12 depths from 1,000 m to the surface (comprising the three sampling depths for plankton diversity) and filtered onto precalcined (24 h, 450°C) GF/F filters. Blanks were measured at each station by filtering 2 L of milliQ water. Filters were stored into precalcined glass vials and dried in an oven (24 h, 50°C). Back in the laboratory, samples were fumigated with pure HCl (24 h) to dissolve the carbonate fraction. The analysis of carbon was performed on a CHN analyzer (Perkin-Elmer 2400) calibrated with acetanilide. POC measurements were not corrected for possible DOC adsorption on the filter. The limit of detection (defined as three time the standard deviation of the blanks for the entire cruise) was 0.2 mmol m^{-3}.

2.2. Partial Least Square Regression: Training and Testing

Partial least square regression (PLSR) is a statistical multivariate regression model that allows regressing a matrix of response variables (Y, here $\%C_{group}$) on a predictor matrix (X, here the hydrological and optical data). Its main interest is to decompose the data into principal components that best summarize both X and Y prior to the regression (Abdi, 2010). This technique prevents the bias induced by collinearity that is often observed in ecological data (e.g., co-occurence of species). The data used as predictors were depth, temperature, salinity, Chl, b_{bp}, c_p, and the ratios Chl:b_{bp}, Chl:c_p, and b_{bp}:c_p (supporting information Table S2). Because of the small amount of data used to train the PLSR (33 samples), a single cross-validation was not sufficient to estimate the quality of the prediction. A bootstrapping technique was used by randomly splitting the data set into learning (2/3) and testing (1/3) subsets and calculating the coefficient of determination (R^2) and the root mean square error (RMSE) of the prediction. This procedure was repeated

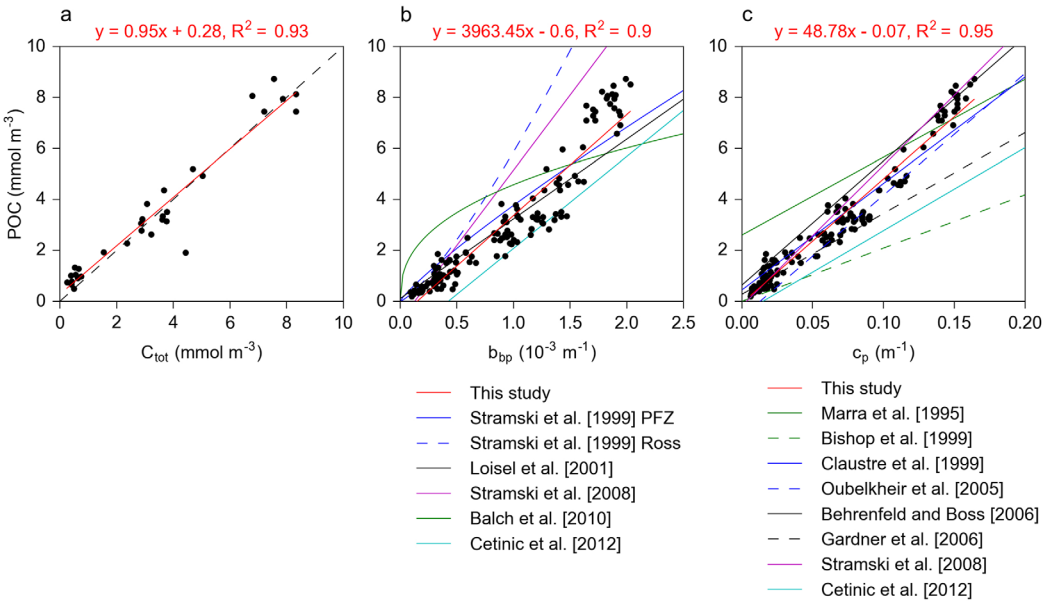

Figure 3. Relationship between (a) total calculated plankton carbon (C_{tot}) versus measured POC (n = 33), the dotted line denotes the 1:1 relationship, (b) b_{bp} versus POC (n = 156), and (c) c_p versus POC (n = 156) during the SOCLIM cruise (red line). In Figures 3b and 3c, relationships from previous studies are shown for a comparison (PFZ and Ross refer to two different fits for the Polar Frontal Zone and Ross sea in Stramski et al. 1999).

10 000 times and statistics were derived from the predictions ensemble (Table 2 and supporting information Figure S1).

In this study we selected five BGC-Argo floats equipped with pressure, temperature, salinity, F, b_{bp} (700 nm), c_p (650 nm), and downward irradiance at 490 nm ($E_{d\ (490)}$) sensors (Wet Labs ECO triplet, Wet Labs C-rover) in the vicinity of the area where the PLSR was trained (Figures 1b and 1c), two of them being deployed during the SOCLIM cruise. Float data were downloaded from the global Argo database (Argo, 2017) accessible at ftp://ftp.ifremer.fr/ifremer/argo/. Prior to the prediction, the F, b_{bp} and c_p data from the floats were treated in the same way as the ship data (conversion from raw data, correction of fluorescence quenching and low-pass filtering for spikes removal, see section 2.1). Additionally, the c_p sensor drift was corrected by subtracting the deep signal (1,000 m) from each profile. Finally, the fluorescence values (F) were calibrated into chlorophyll *a* concentration (Chl) using $E_{d\ (490)}$ and a previously published optical model (Xing et al., 2011).

$$Chl = F_{490} \cdot F$$

A median F_{490} value was calculated for each float (supporting information Figure S2) and used to convert F data into Chl for the whole float record. The mixed layer depth (MLD) was calculated using the density-difference criteria (0.03 kg m^{-3} compared to the density at 20 m, de Boyer Montégut et al., 2004). The contribution of each plankton group to total plankton carbon ($\%C_{group}$) was predicted for each float profile between 0 and 250 m using the PLSR trained with the SOCLIM cruise data.

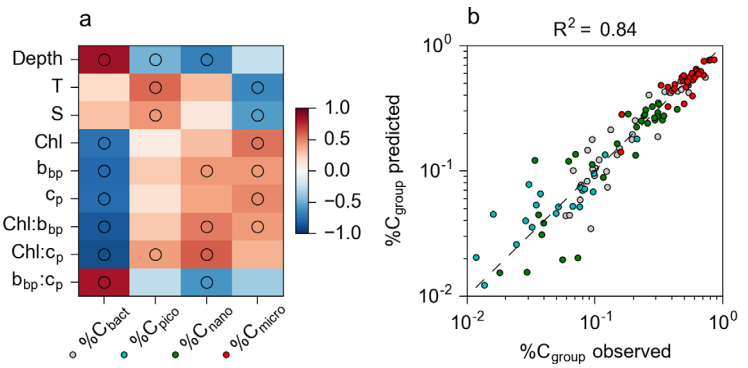

Figure 4. (a) Heatmap of the correlation coefficients between the relative contribution of each plankton group to C_{tot} ($\%C_{group}$) and the hydrological and optical data collected during the SOCLIM cruise. Highly significant coefficients ($p < 0.01$) are specified by a circle (same color code as in Fig. 2). (b) Contribution of each plankton group to C_{tot} as predicted by the PLSR compared to the observations.

2.3. Independent Quantification of Large Particle Abundance and Particle Size From the Float Data

Spikes in the fluorescence and backscattering signals are attributed to large particles (Briggs et al., 2011). Spikes were identified by subtracting the low-pass filtered data to the raw (not unspiked) data (Briggs et al., 2011). The number of b_{bp} spikes below 250 m was quantified by counting the number of events with a height exceeding 0.001 m^{-1} . Events with values >0.004 m^{-1} were attributed to

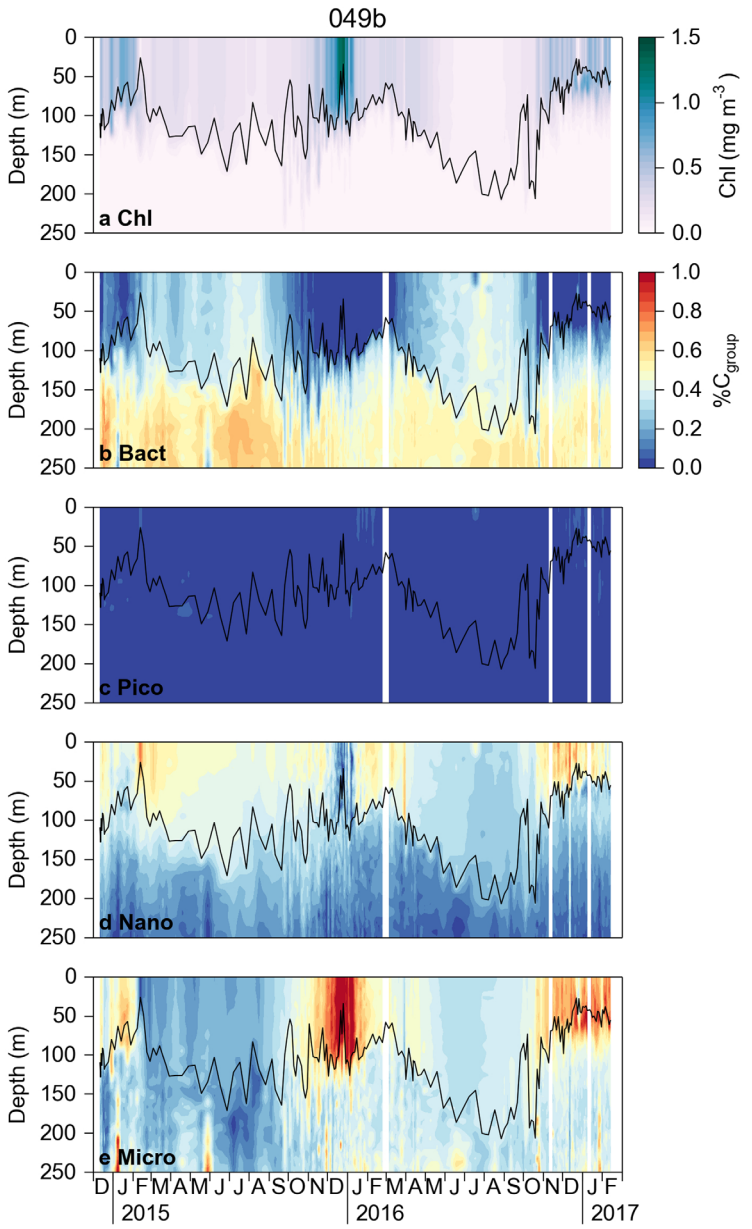

Figure 5. a) Section of chlorophyll *a* concentration (Chl) and (b-e) contribution of each plankton group to C_{tot} as predicted by the PLSR for float 049b. Black line represents the mixed layer depth.

large motile organisms and discarded from the enumeration. Similarly, a threshold of 0.2 mg m^{-3} was selected to quantify the chlorophyll *a* fluorescence spikes. These thresholds were determined empirically after the careful examination of numerous profiles. The total number of for both b_{bp} and fluorescence was normalized by the total number of data points below 250 m (depth of the winter mixed layer) to take into account the change in the vertical sampling resolution between summer and winter. Thereby, percentages of both b_{bp} and fluorescence spikes are provided for each float profile.

The mean diameter of particles contributing to c_p in the upper layer (10–50 m) was calculated following Briggs et al. (2013). This depth interval is always in the mixed layer and was chosen to take advantage of the higher recording frequency (1 data per meter) in the first 50 meters to quantify the variance of the c_p signal and avoid the influence of swell potentially injecting bubbles and/or affecting the float ascent speed in the first 10 meters. Briefly, each raw (not unspiked) c_p profile was de-trended by subtracting an 11-point running median to isolate the high-frequency variability due to random fluctuations in particle concentration within the sample volume. Values of detrended c_p exceeding 0.066 m^{-1} were removed in order to eliminate very large particles (>2 mm diameter) from the analysis that are too rare to be sampled reliably (Briggs et al., 2013). Additionally, the highest remaining detrended c_p value from each profile was removed to further reduce random variability due to large and rare particles. Mean particle diameter d_{ML} (weighted by contribution to c_p) was calculated in the 10–50 m depth interval following Eq. (1).

$$\bar{A}_{cp} = \frac{var\left(c_{p\,detrended}\right)}{mean\left(c_p\right)} \cdot \frac{V}{Q_c} \cdot \frac{1}{\alpha(\tau)} \tag{1}$$

$$\alpha(\tau) = \begin{cases} 1-(3\tau)^{-1} \, if \, \tau \geq 1 \\ \tau - \tau^2/3 \, if \, \tau \leq 1 \end{cases}$$

$$\tau = \left(\frac{t_{res}}{t_{samp}}\right)$$

$$d_{ML} = 2\sqrt{\bar{A}_{cp}\pi^{-1}}$$

where $var(c_{p\_detrended})$ is the variance of the detrended c_p signal, $mean(c_p)$ is the mean of the raw c_p signal (large spikes removed), V is the sample volume (12.5 ml), Q_c is the attenuation efficiency (2 for particles much larger than the wavelength of light, Bohren & Huffman, 1983), and α is a correction for the increase in effective sample volume due to water movement. α was calculated from a sample integration time t_{samp} of 1 s and a particle residence time t_{res} of 0.1 s, based on 10 cm s^{-1} movement speed of water through the sample volume and a mean path of 1 cm.

3. Results and Discussion

3.1. Plankton Carbon Estimation and Performance of the Prediction

Despite a general dominance of microplankton to the total plankton biovolume (>80% in all samples, Figure 2a), its contribution to C_{tot} was generally lower (Figure 2b), reflecting a lower carbon content for this plankton group (Menden-Deuer & Lessard 2000; Table 1). Deep samples (250 m) were characterized by low POC concentration (<1 mmol m^{-3}, supporting information Table S1) and a strong bacterial (including

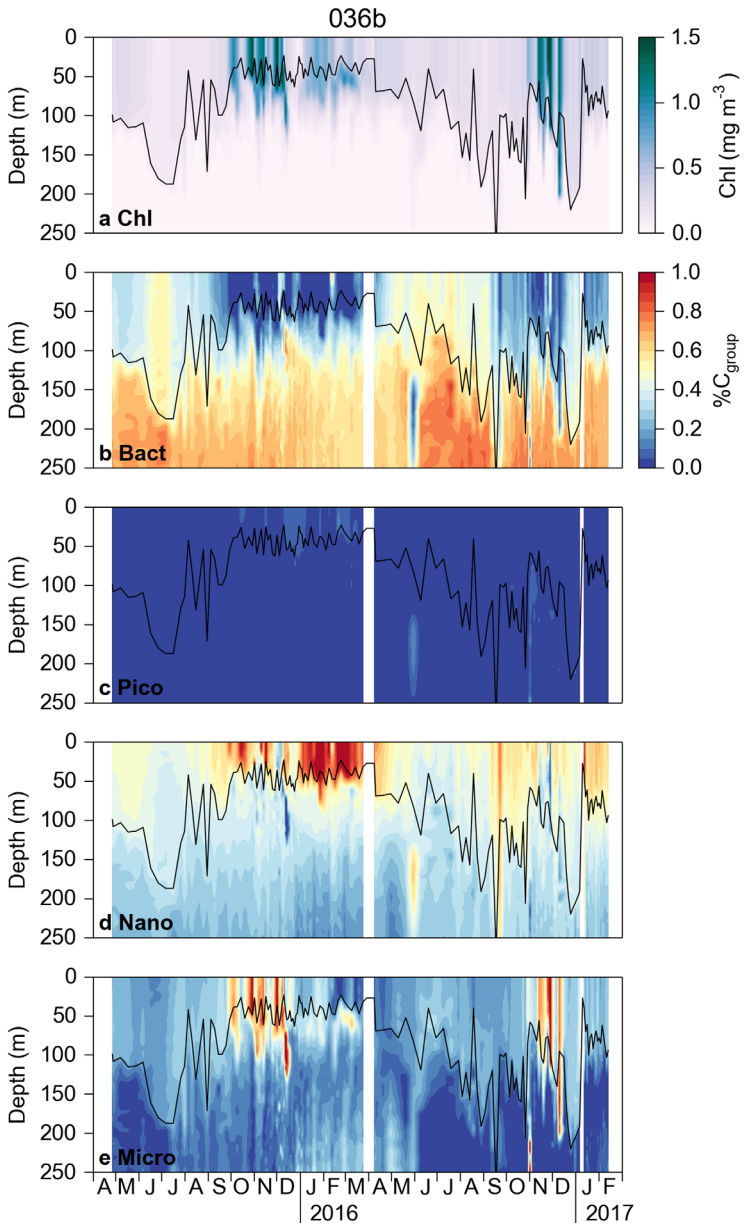

Figure 6. Same as Figure 5 for float 036b.

Bacteria and Archaea) contribution to C_{tot} (30–70%, Figure 2b). Nanoplankton showed an important contribution to C_{tot} (30–50%) at 100 m and 10 m at all stations except TNS08 and A3_2 where microplankton clearly dominated C_{tot} (~80%). Both stations were characterized by Chl >1 mg m^{-3} and the presence of typically bloom-forming diatoms (e.g., *Chaetoceros curvisetus*, *Eucampia antarctica*, supporting information data set), suggesting a recent initiation of the spring bloom (Korb et al., 2012; Lasbleiz et al., 2016). Picoplankton contribution was low in all samples (<20%). The linear relationship between C_{tot} and the measured POC with a slope of ~1 (Figure 3a) suggests that plankton cells were correctly enumerated and that carbon content values from the literature are appropriate to estimate plankton carbon partitioning in relatively contrasted provinces of the SO (from the Subantarctic Zone, SAZ to the Antarctic Zone, AAZ). Furthermore, it implies that detritus and non-living particles that were not quantified here represent a minor fraction of the POC at the time of the sampling in early spring. Although this hypothesis is plausible, it must be stressed that plankton carbon estimation depends critically on the cell carbon content or the carbon:volume relationships that are selected (Table 1). These relationships are often associated with important natural variability (>50%) related to the cell physiological status and life cycle (Menden-Deuer & Lessard, 2000).

The relationships between b_{bp} and POC and c_p and POC lay between those previously reported from various locations of the ocean, and the fit of POC versus b_{bp} showed a lower R^2 than that of POC versus c_p (Figures 3b and 3c). This feature has been reported before and is indicative of changes in backscattering efficiency with the nature of particles (Cetinić et al., 2012; Stramski et al., 1999). For example, smaller particles associated with the lower POC concentrations would have a higher refractive index (Morel & Ahn, 1991). For this reason, POC was predicted from the c_p values reported by the floats, rather than b_{bp}. Here, we first investigated the relationships between hydrological/optical properties and plankton groups by using simple linear correlations (Figure 4a). Bacteria were significantly correlated with all optical variables, and more specifically positively correlated to the b_{bp}:c_p ratio, generally thought to increase with an increasing abundance of small particles ~1 μm (Morel & Ahn, 1991; Stramski & Kiefer, 1991). Microplankton was significantly and positively correlated with Chl, proxies of particle abundance (c_p and b_{bp}) and the Chl:b_{bp} ratio. This observation is consistent with a previous study in the sub-polar North Atlantic that also associated high diatom biomass with elevated Chl:b_{bp} ratios (Cetinić et al., 2015).

To quantitatively predict the contribution of each plankton group to C_{tot}, we successfully trained and validated the PLSR model using the bootstrapping technique. The RMSE was not homogeneous between plankton groups and ranged from 14% for bacteria to 26% for picoplankton (Table 2). These results generally give confidence in the multivariate regressive model, which allows us to apply the method on data collected by five BGC-Argo floats covering a large section of the Indian Sector of the SO.

3.2. Spatial and Seasonal Patterns of Plankton Community Structure From BGC-Argo Floats Data

Float 049b was located upstream of the Kerguelen Plateau, mainly in the AAZ (Figure 1c). Float 036b drifted north of the Crozet and Kerguelen Plateaus in the Polar Frontal Zone (PFZ). Float 037c presented a long trajectory downstream of the Kerguelen Plateau, crossing the Polar Front and Subantarctic Front. Floats 107c

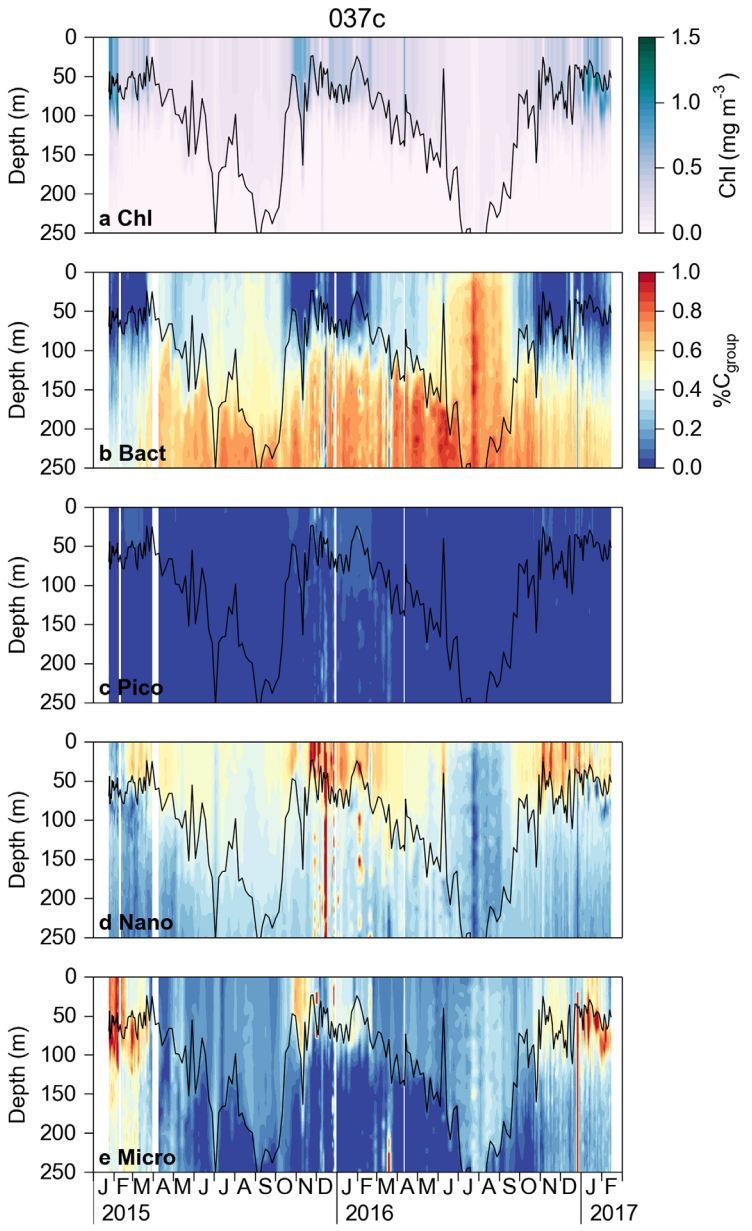

Figure 7. Same a Figure 5 for float 037c.

and 104c were respectively deployed at the SOCLIM stations FS (upstream of the Kerguelen Plateau, low biomass) and TNS08 (Downstream of the Kerguelen Plateau, High biomass) in the AAZ (Figure 1b).

$\%C_{bact}$ was generally high below the MLD (>50%) and relatively high in winter in the mixed layer (25–50%, Figures 5b–7b). Conversely, it was negligible during phytoplankton blooms. This is consistent with the inverse relationship between phytoplankton and heterotrophic bacteria contributions to total carbon observed in the global ocean (Simon et al., 1992). Although it has been demonstrated that the abundance of heterotrophic bacteria can increase drastically during phytoplankton blooms in the SO and contribute to nutrient recycling (Christaki et al., 2014; Obernosterer et al., 2008; Pearce et al., 2011), the corresponding carbon biomass is generally <1 μmol L^{-1}. However, a rapid increase of $\%C_{bact}$ (up to 50%) was observed after the phytoplankton blooms recorded by floats 036b (Figure 6b, May 2016) and 037c (Figure 7b, April 2015), reflecting the increasing contribution of bacterial biomass in the mixed layer independently from MLD deepening. $\%C_{pico}$ was negligible for floats located in the AAZ (Figures 5c, 8c, and 9c) and reached ~10% in the mixed layer in summer 2015–2016 for floats 036b (Figure 6c) and 037c (Figure 7c) when they occupied the Northernmost location of their drift (PFZ to SAZ). A strong southward decrease in picoplankton abundance was previously reported from the Subtropical Zone (STZ) to the AAZ (Díez et al., 2004) and picoplankton contribution to phytoplankton biomass is generally <5% in productive environments of the SO (Díez et al., 2004; Lasbleiz et al., 2014; Uitz et al., 2009). $\%C_{nano}$ showed highest values (>80%) in the mixed layer North of the Crozet Plateau (January–March 2016, float 036b, Figure 6d) and upstream of the Kerguelen Plateau in October 2016 and January 2017 (float 107c, Figure 8d). High nanoplankton biomass was previously reported at the end of the North Crozet phytoplankton bloom dominated by *Phaeocystis antarctica* (Poulton et al., 2007). Additionally, the phytoplankton community on the western flank of the Kerguelen Plateau is characterized by a dominance at an annual scale of prasinophytes and prymnesiophytes, out of the diatom bloom (Fiala et al., 1998). Floats 036b, 049b and 037c reported elevated $\%C_{nano}$ (>40%) in autumn concomitantly with the deepening of the MLD (from ~50 to >100 m). This succession from microplankton dominance in summer to nanoplankton dominance when vertical mixing increases is generally observed in situ (Arrigo et al., 1999; Goffart et al., 2000; Mangoni et al., 2004; Uitz et al., 2009) and also suggested from phytoplankton groups based on predictions from satellite-derived observations (Alvain et al., 2008).

All the floats located in the AAZ reported elevated Chl (>1 mg m^{-3}) with a concomitant dominance (>80%, Figures 5e, 8e, and 9e) of microplankton. Diatoms dominated the microplankton counts and biomass in the SOCLIM data set used to train the PLSR (supporting information data set). It is likely that the strong microplankton dominance predicted from the float data reflects a major diatom contribution as usually observed in productive environments of the SO (Armand et al., 2008; Korb et al., 2012; Lasbleiz et al., 2016; Rembauville et al., 2016a). Floats 107c and 104c, respectively deployed at low- and high biomass sites in the vicinity of the Kerguelen Plateau, clearly reported the succession from a dominance of nano- to microplankton during the spring/summer phytoplankton bloom (Figures 8 and 9). However, in November, the microplankton

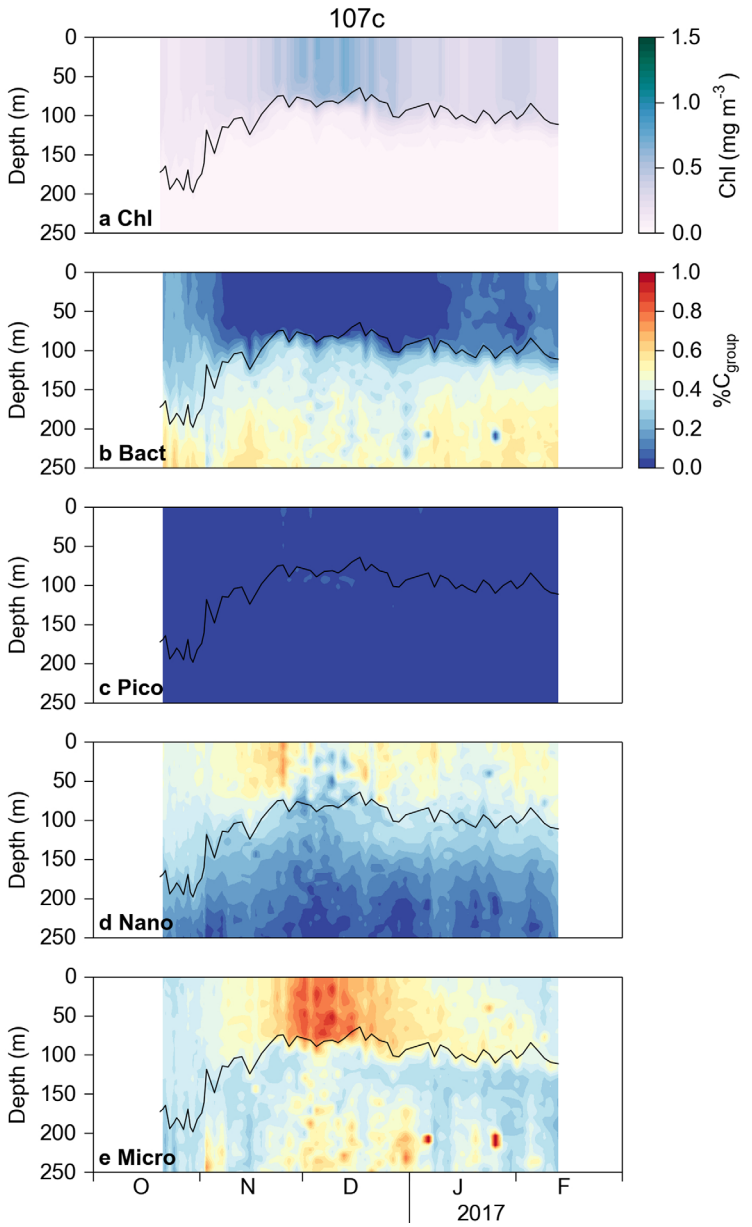

Figure 8. Same a Figure 5 for float 107c.

contribution was higher downstream of the Kerguelen Plateau (>90%, Figure 9d) when compared to upstream (50–80%, Figure 8d). This observation is likely attributed to the higher iron availability downstream of the Kerguelen Plateau (Blain et al., 2008; Quéroué et al., 2015) that supports a phytoplankton bloom clearly dominated by diatoms (Armand et al., 2008; Lasbleiz et al., 2016). Moreover, float 104c reported a patch of microplankton biomass in December below the mixed layer (150–200 m, Figure 9d). This could be interpreted as the export of diatoms at the end of the bloom resulting from aggregation or other ecological processes (e.g., resting spore formation) as previously described in this area (Laurenceau-Cornec et al., 2015; Rembauville et al., 2015). Particle detrainment associated with the shoaling of the MLD could also explain the presence of phytoplankton biomass below the mixed layer (Dall'Olmo et al., 2016).

The mean particle diameter within the mixed layer (d_{ML}, estimated from high frequency c_p variability) ranged 15 – 500 μm (Figure 10). It represents an average of idealized spherical particles that hides an important diversity of particles sizes and shapes in the ocean (e.g., parallelepiped pennate to spiny centric diatoms, in single cells or chains, spherical to tabular faecal pellets). However, although d_{ML} showed high variability at short time scale, the values and seasonal patterns are broadly consistent with the POC dynamics and the predicted plankton community structure. Lowest d_{ML} (15–50 μm) was preferentially observed in winter when $\%C_{micro}$ was low and $\%C_{nano}$ was relatively high. This value might be considered as an average for the abundant nanoplankton (<20 μm) and the typically dominant small microplankton in winter such as *Thalassionema nitzschioides* (<20 μm) and *Fragilariopsis kerguelensis* (~40 μm for single cells) (Rembauville et al., 2015, 2016b; Rigual-Hernández et al., 2015). By contrast, the highest d_{ML} values (200 - 500 μm) were observed in summer during high POC, microplankton-dominated phytoplankton blooms. These blooms are generally composed of a mixture of chain forming (chain length >100 μm) small diatoms (*Pseudo-Nitzschia*, *Chaetoceros Hyalochaete, Odontella*), large diatoms such as *Corethron pennatum* (200 μm), *Proboscia* and *Rhizosolenia* (200–500 μm), large dinoflagellates (*Protoperidinium*, *Gyrodinium* ~100 μm) and even the giant diatom *Thalassiothrix* (>1,000 μm length) (Armand et al., 2008; Kopczyńska et al., 1998; Lasbleiz et al., 2016; Rembauville et al., 2016a). Interestingly, the late summer nanoplankton-dominated bloom North of Crozet was not associated with any increase in d_{ML} that remained <50 μm (float 036b, January–March 2016, Figure 10b). This observation further supports the interpretation of the predicted high $\%C_{nano}$ and elevated Chl as a potential indicator of *Phaeocystis* presence as both colony-bound and colony-free cells in the late summer North Crozet Bloom (Poulton et al., 2007).

Despite the generally good agreement between the predicted carbon partitioning, the mean particle diameter estimate, and the literature data, this approach has some limitations which need to be addressed. First, the PLSR prediction has a RMSE of 14–26% depending on the considered plankton group. In the case of picoplankton, the RMSE is larger than the highest predicted values (~10%). Second, the PLSR was trained on a limited range of hydrological and optical data. Despite having selected BGC-floats with trajectories included in the same zones as the SOCLIM stations, occasionally the float data could be outside the range of variables used for training the PLSR. Should the PLSR be used in such situations, this would potentially

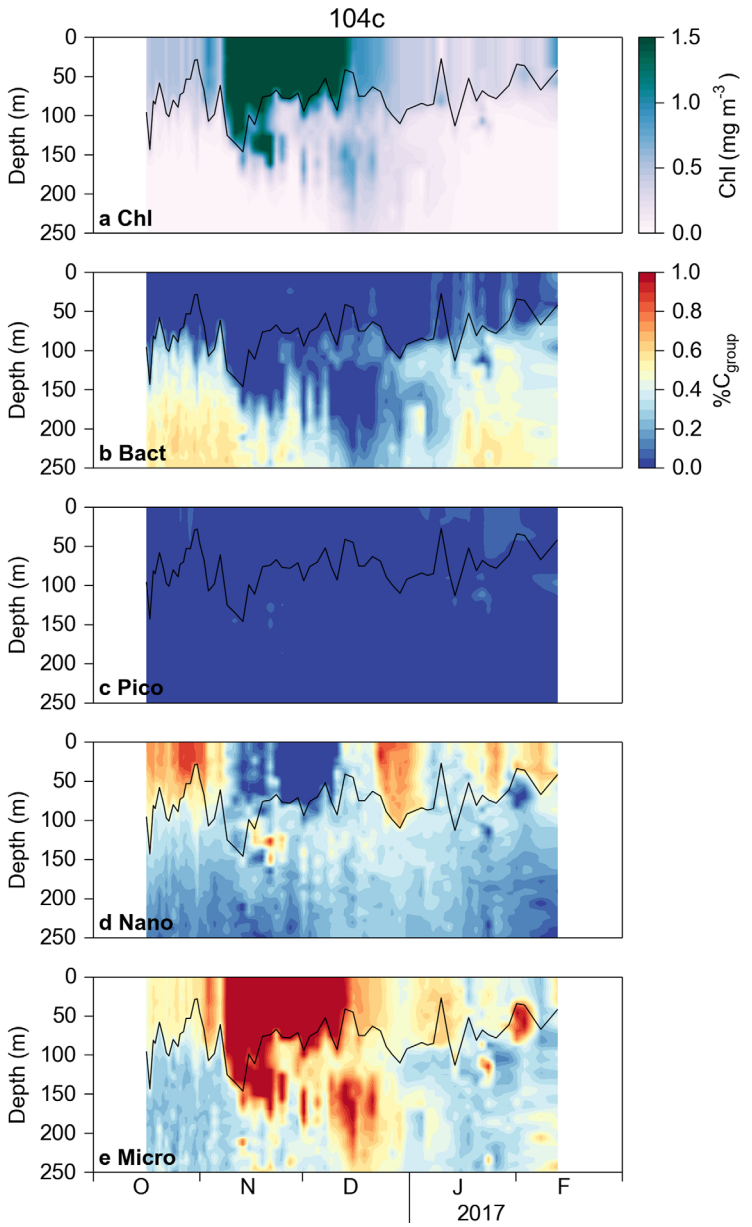

Figure 9. Same a Figure 5 for float 104c.

lead to over/underestimation of $\%C_{group}$ (e.g., the predicted $\%C_{group}$ might be slightly <0 or >1, supporting information Figure S3). Finally, the PLSR was calibrated with spring data when non-living, detrital POC is likely to be a minor fraction of total POC (reflected by a close to null intercept in the regression presented in Figure 3a). The prediction in summer and autumn cannot account for this non-living POC fraction, and the resulting view of the plankton community is probably biased (e.g., underestimation of the importance of heterotrophic protists at the end of the bloom, Pearce et al., 2011; Christaki et al., 2014). For these reasons, only broad seasonal and geographical trends of the predicted $\%C_{group}$ can be discussed and absolute values should be carefully compared to measurements from classical sampling. Despite these limitations, except from localized coastal or neritic studies (e.g., Jeandel et al., 1998; Moline & Prézelin, 1996), this approach provides insights into seasonal and geographical shifts in oceanic plankton community composition in the SO at an unprecedented temporal and spatial resolution. Additional data of bio-optical signals and plankton community composition collected during other seasons (summer, autumn and winter) in the same biological province would certainly increase the quality of the prediction by improving the PLSR training and the cross-validation procedure.

3.3. Mixed Layer Community Structure and Particles Dynamics in the Mesopelagic Ocean

Local studies have already demonstrated that plankton assemblage shapes the magnitude and stoichiometry of export fluxes (Rembauville et al., 2015; Salter et al., 2012), but there is a need for a better understanding of the relationship observed at a global scale between plankton community structure in the upper layers, export intensity and transfer efficiency into the deep ocean (Guidi et al., 2015; Henson et al., 2012). The high spatial and temporal resolution of the floats data and the biomass and community gradients observed here allow us to study the relationship between mixed layer plankton community composition and proxies of export (large particles diagnosed from b_{bp} and F spikes below 250 m).

A low occurrence of b_{bp} spikes below 250 m ($<1\%$) was observed in autumn and winter when $\%C_{nano}$ was high (Figure 10). Conversely, an increase in the b_{bp} spikes (up to 2%) occurred when microplankton dominated the mixed layer community composition. Fluorescence spikes showed different patterns than b_{bp} spikes and were specifically associated with high biomass (POC >10 mmol m^{-3}) and microplankton-dominated conditions as seen by float 036b in October-December 2015 (Figure 10b), float 037c in January–February 2015 (Figure 10c) and float 104c in December 2016 (Figure 10e). Spikes in the b_{bp} signal are generated by large particles (order of magnitude 1 mm, Briggs et al., 2011), likely attributed to faecal pellets and/or phytoaggregates. Zooplankton grazing affects the composition of phytoplankton pigments and notably removes Mg^{2+} from chlorophyll *a*, hence resulting in the accumulation of non-fluorescent phaeopigments in the faecal pellets (Downs & Lorenzen, 1985). Conversely, in the case of phytoplankton senescence in the upper ocean, the degradation of the phytyl chain of the chlorophyll *a* (Rontani et al., 1995) does not impact the fluorescence of the chlorin ring. Thus, the b_{bp} and fluorescence spikes occurrence in the mesopelagic ocean might reflect respectively the presence of zooplankton faecal pellets (or other particles from heterotrophic origin) or relatively fresh phytoplankton aggregates and senescent cells that were not subject to grazing. Float 104c reported a 1 month lag between the high occurrence of b_{bp} spikes in November and fluorescence spikes in December (Figure 10e). Moreover,

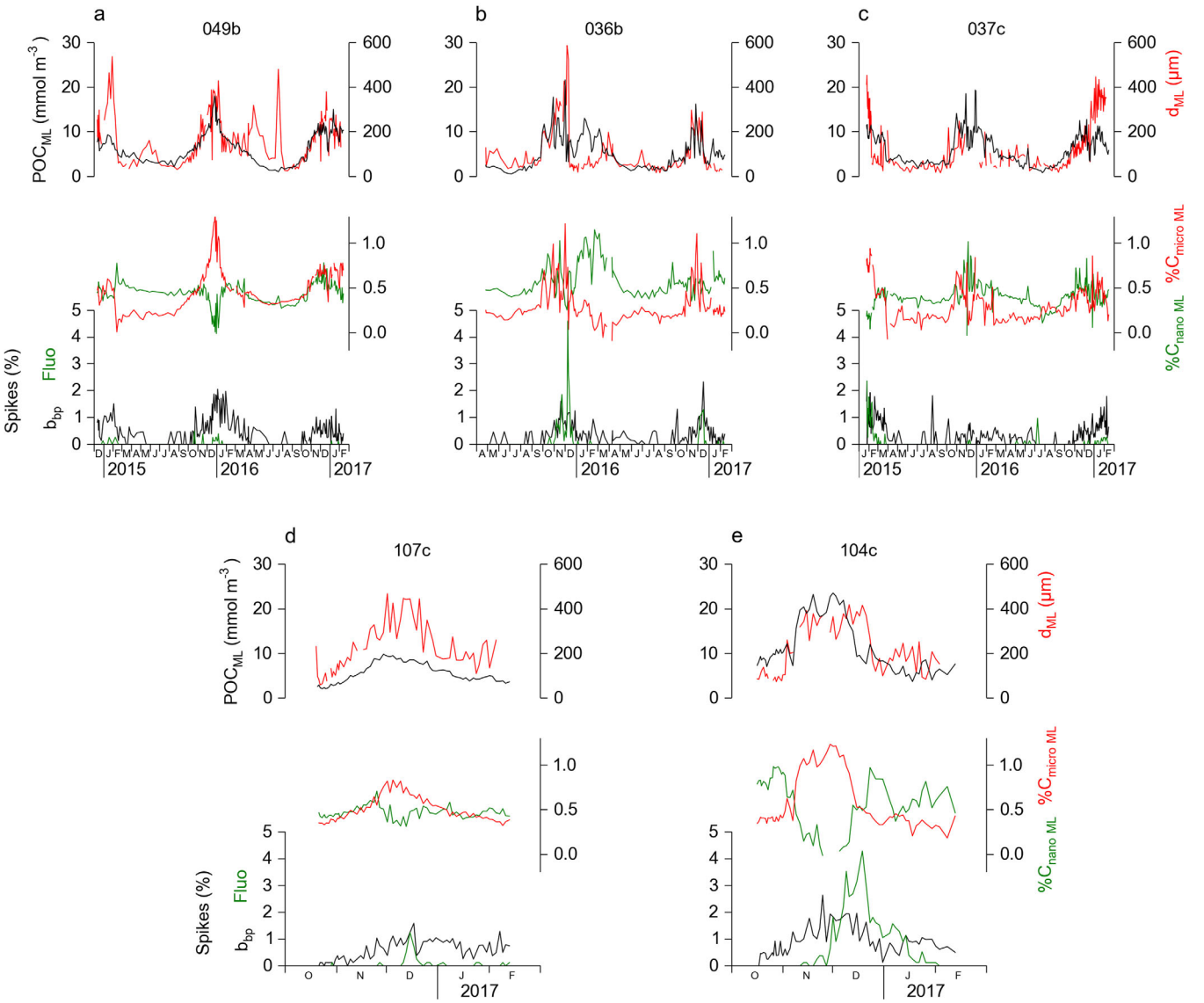

Figure 10. Mean POC in the mixed layer (POC_{ML}), mean particles diameter in the mixed layer (d_{ML}), mean contribution of nano- and microplankton to total plankton carbon in the mixed layer, and occurrence of b_{bp} and fluorescence spikes below 250 m for the five BGC-Argo floats.

the period of high fluorescence spikes below 250 m was concomitant with and restricted to the presence of a microplankton patch predicted below the mixed layer in December (Figure 9e). By contrast, the period of significant presence of b_{bp} spikes extends from October to late January. These observations can be tentatively interpreted as the signature of a temporal evolution in the relative dominance of different export vectors: zooplankton faecal pellets during the initiation, apex and decline of microplankton bloom and phytoaggregates only associated with the decline of the bloom. A temporal coupling between phytoplankton bloom and faecal pellet export has already been reported in productive areas of the Southern Ocean (Manno et al., 2015; Rembauville et al., 2015). It might be explained by the elevated sinking speed of faecal pellets that are exported concomitantly with zooplankton grazing in the mixed layer (typically >100 m d^{-1}; Smayda, 1969). The sinking of phytoplankton aggregates might result from nutrient limitation at the end of the phytoplankton bloom (Thornton, 2002). Given the higher sinking speed and the mechanical protection of the faecal pellets, they might be associated with a high transfer efficiency to the mesopelagic ocean (Cavan et al., 2017). However, because of the very different composition and sinking speed of these export vectors, the carbon export fluxes associated with the b_{bp} and fluorescence spikes cannot be quantified here.

4. Conclusion

During the SOCLIM cruise, plankton carbon was partitioned among bacteria, pico-, nano- and microplankton and the associated hydrological and optical parameters were collected. Based on a statistical multivariate regression, the carbon partitioning between these plankton groups can be reasonably estimated from the hydrological and optical properties. This allows a prediction of plankton carbon partitioning based on BGC-Argo float data located in the vicinity of ship-based observations. The seasonal and geographical patterns of the predicted plankton carbon partitioning appears consistent with literature data and agree with an independent estimate of the mean particles size within the mixed layer based on high frequency c_p variability.

This methodology can be used to address specific biogeochemical questions such as the impact of plankton community structure on the distribution of particles in the upper mesopelagic. Microplankton-dominated conditions lead to an increase in the occurrence of spikes in the b_{bp} signal in the mesopelagic attributed to large particles such as faecal pellets. More specifically, intense microplankton blooms are associated with the presence of large fluorescent particles below 250 m interpreted as the export of fresh phytoaggregates. These results suggest that microplankton blooms of high magnitude might lead to the export of relatively fresh large particles below the winter mixed layer depth.

Thanks to the acquisition of a dedicated data set allowing relationships between plankton composition and optical proxies to be established, this study emphasizes the potential of profiling floats to propagate these relationships in space and time over the float life-time. In the SO, climate change is likely to impact the plankton community structure (Alvain et al., 2013; Boyd et al., 2016; Davidson et al., 2016; Petrou et al., 2016) and long observational time series are currently missing to document such changes. Autonomous platforms are powerful tools that can document important ecological and biogeochemical processes currently under-sampled by classical ship-based oceanographic cruises. Together with local biologically-resolved studies and other float-based estimates of carbon fluxes (Estapa et al., 2017) or chemical parameters (Sauzède et al., 2017), this approach allows to fill observational gaps and might help to document at large scale potential shifts in plankton community structure and the associated changes in the functioning of the biological pump.

Acknowledgments
We thank the captain V. Broi and the crew of the R/V *Marion Dufresne II* for their support aboard. We thank people from DT-INSU and IPEV for the excellent technical support during the cruise and Audrey Guéneuguès and Pavla Debeljak for the collection of the samples for flow cytometry. This work is part of the project SOCLIM (Southern Ocean and climate) supported by the French research program LEFE-CYBER of INSU-CNRS, the Climate Initiative of the foundation BNP Paribas, the French polar institute (IPEV), the European Research Council (remOcean project, grant agreement 246777), and the Université Pierre et Marie Curie. These data were collected and made freely available by the International Argo Program and the national programs that contribute to it (http://www.argo.ucsd.edu, http://argo.jcommops.org). The Argo Program is part of the Global Ocean Observing System.

References

Abdi, H. (2010). Partial least squares regression and projection on latent structure regression (PLS Regression). *Wiley Interdisciplinary Reviews: Computational Statistics*, *2*(1), 97–106. https://doi.org/10.1002/wics.51

Alvain, S., Le Quéré, C., Bopp, L., Racault, M.-F., Beaugrand, G., Dessailly, D., & Buitenhuis, E. T. (2013). Rapid climatic driven shifts of diatoms at high latitudes. *Remote Sensing Environment*, *132*, 195–201. https://doi.org/10.1016/j.rse.2013.01.014

Alvain, S., Moulin, C., Dandonneau, Y., & Loisel, H. (2008). Seasonal distribution and succession of dominant phytoplankton groups in the global ocean: A satellite view. *Global Biogeochemical Cycles*, *22*, GB3001. https://doi.org/10.1029/2007GB003154

Ardyna, M., Claustre, H., Sallée, J.-B., D'ovidio, F., Gentili, B., van Dijken, G., . . . Arrigo, K. (2017). Delineating environmental control of phytoplankton biomass and phenology in the Southern Ocean. *Geophysical Research Letters*, *44*, 5016–5024. https://doi.org/10.1002/2016GL072428

Argo (2017). *Argo float data and metadata from Global Data Assembly Centre (Argo GDAC)––Snapshot of Argo GDAC of February, 8st 2017*. SEANOE. https://doi.org/10.17882/42182

Armand, L. K., Cornet-Barthaux, V., Mosseri, J., & Quéguiner, B. (2008). Late summer diatom biomass and community structure on and around the naturally iron-fertilised Kerguelen Plateau in the Southern Ocean. *Deep Sea Research Part II: Topical Studies in Oceanography*, *55*(5–7), 653–676. https://doi.org/10.1016/j.dsr2.2007.12.031

Arrigo, K. R., Robinson, D. H., Worthen, D. L., Dunbar, R. B., DiTullio, G. R., VanWoert, M., & Lizotte, M. P. (1999). Phytoplankton community structure and the drawdown of nutrients and CO_2 in the Southern Ocean. *Science*, *283*(5400), 365–367. https://doi.org/10.1126/science.283.5400.365

Arrigo, K. R., van Dijken, G. L., & Bushinsky, S. (2008). Primary production in the Southern Ocean, 1997–2006. *Journal of Geophysical Research*, *113*, C08004. https://doi.org/10.1029/2007JC004551

Balch, W. M., Bowler, B. C., Drapeau, D. T., Poulton, A. J., & Holligan, P. M. (2010). Biominerals and the vertical flux of particulate organic carbon from the surface ocean. *Geophysical Research Letters*, *37*, L22605. https://doi.org/10.1029/2010GL044640

Behrenfeld, M. J., & Boss, E. (2003). The beam attenuation to chlorophyll ratio: An optical index of phytoplankton physiology in the surface ocean? *Deep Sea Research Part I:Oceanographic Resesearch Papers*, *50*(12), 1537–1549. https://doi.org/10.1016/j.dsr.2003.09.002

Behrenfeld, M. J., & Boss, E. (2006). Beam attenuation and chlorophyll concentration as alternative optical indices of phytoplankton biomass. *Journal of Marine Research*, *64*(3), 431–451. https://doi.org/10.1357/002224006778189563

Bishop, J. K. (1999). Transmissometer measurement of POC. *Deep Sea Res. Part I: Oceanographic Research Papers*, *46*(2), 353–369. https://doi.org/10.1016/S0967-0637(98)00069-7

Bishop, J. K. B., Wood, T. J., Davis, R. E., & Sherman, J. T. (2004). Robotic Observations of Enhanced Carbon Biomass and Export at 55S During SOFeX. *Science*, *304*(5669), 417–420. https://doi.org/10.1126/science.1087717

Blain, S., Sarthou, G., & Laan, P. (2008). Distribution of dissolved iron during the natural iron-fertilization experiment KEOPS (Kerguelen Plateau, Southern Ocean). *Deep Sea Research Part II: Topical Studies in Oceanography*, *55*(5–7), 594–605. https://doi.org/10.1016/j.dsr2.2007.12.028

Bohren, C. F., & Huffman, D. R. (1983). *Absorption and scattering of light by small particles* (new ed.). New York: John Wiley & Sons.
Boyd, P. W., Arrigo, K. R., Strzepek, R., & van Dijken, G. L. (2012). Mapping phytoplankton iron utilization: Insights into Southern Ocean supply mechanisms. *Journal of Geophysical Research*, *117*, C06009. https://doi.org/10.1029/2011JC007726
Boyd, P. W., Dillingham, P. W., McGraw, C. M., Armstrong, E. A., Cornwall, C. E., Feng, Y., . . . Nunn, B. L. (2016). Physiological responses of a Southern Ocean diatom to complex future ocean conditions. *Nature Climate Change*, *6*(2), 207–213. https://doi.org/10.1038/nclimate2811
Boyd, P. W., & Newton, P. P. (1999). Does planktonic community structure determine downward particulate organic carbon flux in different oceanic provinces? *Deep Sea Research Part I: Oceanographic Research Papers*, *46*(1), 63–91. https://doi.org/10.1016/S0967-0637(98)00066-1
Bratbak, G. (1985). Bacterial biovolume and biomass estimations. *Applied Environmental Microbiology*, *49*(6), 1488–1493.
Briggs, N., Perry, M. J., Cetinić, I., Lee, C., D'asaro, E., Gray, A. M., & Rehm, E. (2011). High-resolution observations of aggregate flux during a sub-polar North Atlantic spring bloom. *Deep Sea Research Part I: Oceanographic Research Papers*, *58*(10), 1031–1039. https://doi.org/10.1016/j.dsr.2011.07.007
Briggs, N. T., Slade, W. H., Boss, E., & Perry, M. J. (2013). Method for estimating mean particle size from high-frequency fluctuations in beam attenuation or scattering measurements. *Applied Optics*, *52*(27), 6710–6725. https://doi.org/10.1364/AO.52.006710
Cavan, E. L., Henson, S. A., Belcher, A., & Sanders, R. (2017). Role of zooplankton in determining the efficiency of the biological carbon pump. *Biogeosciences*, *14*(1), 177–186. https://doi.org/10.5194/bg-14-177-2017
Cetinić, I., Perry, M. J., Briggs, N. T., Kallin, E., D'asaro, E. A., & Lee, C. M. (2012). Particulate organic carbon and inherent optical properties during 2008 North Atlantic Bloom Experiment. *Journal of Geophysical Research*, *117*, C06028. https://doi.org/10.1029/2011JC007771
Cetinić, I., Perry, M. J., D'asaro, E., Briggs, N., Poulton, N., Sieracki, M. E., & Lee, C. M. (2015). A simple optical index shows spatial and temporal heterogeneity in phytoplankton community composition during the 2008 North Atlantic Bloom Experiment. *Biogeosciences*, *12*(7), 2179–2194. https://doi.org/10.5194/bg-12-2179-2015
Charalampopoulou, A., Poulton, A. J., Bakker, D. C. E., Lucas, M. I., Stinchcombe, M. C., & Tyrrell, T. (2016). Environmental drivers of coccolithophore abundance and calcification across Drake Passage (Southern Ocean). *Biogeosciences*, *13*(21), 5917–5935. https://doi.org/10.5194/bg-13-5917-2016
Christaki, U., Lefèvre, D., Georges, C., Colombet, J., Catala, P., Courties, C., . . . Obernosterer, I. (2014). Microbial food web dynamics during spring phytoplankton blooms in the naturally iron-fertilized Kerguelen area (Southern Ocean). *Biogeosciences*, *11*(23), 6739–6753. https://doi.org/10.5194/bg-11-6739-2014
Claustre, H., Morel, A., Babin, M., Cailliau, C., Marie, D., Marty, J.-C., . . . Vaulot, D. (1999). Variability in particle attenuation and chlorophyll fluorescence in the tropical Pacific: Scales, patterns, and biogeochemical implications. *Journal of Geophysical Research*, *104*(C2), 3401–3422. https://doi.org/10.1029/98JC01334
Crosta, X., Romero, O., Armand, L. K., & Pichon, J.-J. (2005). The biogeography of major diatom taxa in Southern Ocean sediments: 2. Open ocean related species. *Palaeogeography, Palaeoclimatology, Palaeoecology*, *223*(1–2), 66–92. https://doi.org/10.1016/j.palaeo.2005.03.028
Dall'Olmo, G., Dingle, J., Polimene, L., Brewin, R. J. W., & Claustre, H. (2016). Substantial energy input to the mesopelagic ecosystem from the seasonal mixed-layer pump. *Nature Geoscience*, *9*(11), 820–823. https://doi.org/10.1038/ngeo2818
Davidson, A. T., McKinley, J., Westwood, K., Thomson, P. G., van den Enden, R., de Salas, M., . . . Berry, K. (2016). Enhanced CO_2 concentrations change the structure of Antarctic marine microbial communities. *Marine Ecology Progress Series*, *552*, 93–113. https://doi.org/10.3354/meps11742
de Baar, H. J. W., Buma, A. G. J., Nolting, R. F., Cadée, G. C., Jacques, G., & Tréguer, P. (1990). On iron limitation of the Southern Ocean: Experimental observations in the Weddell and Scotia Seas. *Marine Ecology Progress Series*, *65*, 105–122. https://doi.org/10.3354/meps065105
de Boyer Montégut, C., Madec, G., Fischer, A. S., Lazar, A., & Iudicone, D. (2004). Mixed layer depth over the global ocean: An examination of profile data and a profile-based climatology. *Journal of Geophysical Research*, *109*, C12003. https://doi.org/10.1029/2004JC002378
Diíez, B., Massana, R., Estrada, M., & Pedrós-Alió, C. (2004). Distribution of eukaryotic picoplankton assemblages across hydrographic fronts in the Southern Ocean, studied by denaturing gradient gel electrophoresis. *Limnology and Oceanography Methods*, *49*(4), 1022–1034. https://doi.org/10.4319/lo.2004.49.4.1022
Downs, J. N., & Lorenzen, C. J. (1985). Carbon: Pheopigment ratios of zooplankton fecal pellets as an index of herbivorous feeding. *Limnology and Oceanography*, *30*(5), 1024–1036. https://doi.org/10.4319/lo.1985.30.5.1024
Erickson, Z. K., Thompson, A. F., Cassar, N., Sprintall, J., & Mazloff, M. R. (2016). An advective mechanism for deep chlorophyll maxima formation in southern Drake Passage. *Geophysical Research Letters*, *43*, 10846–10855. https://doi.org/10.1002/2016GL070565
Estapa, M., Durkin, C., Buesseler, K., Johnson, R., & Feen, M. (2017). Carbon flux from bio-optical profiling floats: Calibrating transmissometers for use as optical sediment traps. *Deep Sea Research Part I: Oceanographic Research Papers*, *120*, 100–111. https://doi.org/10.1016/j.dsr.2016.12.003
Fauchereau, N., Tagliabue, A., Bopp, L., & Monteiro, P. M. S. (2011). The response of phytoplankton biomass to transient mixing events in the Southern Ocean. *Geophysical Research Letters*, *38*, L17601. https://doi.org/10.1029/2011GL048498
Fiala, M., Kopczynska, E. E., Jeandel, C., Oriol, L., & Vetion, G. (1998). Seasonal and interannual variability of size-fractionated phytoplankton biomass and community structure at station Kerfix, off the Kerguelen Islands, Antarctica. *Journal of Plankton Research*, *20*(7), 1341–1356. https://doi.org/10.1093/plankt/20.7.1341
Gardner, W. D., Mishonov, A. V., & Richardson, M. J. (2006). Global POC concentrations from in-situ and satellite data. *Deep Sea Research Part II: Topical Studies in Oceanography*, *53*(5–7), 718–740. https://doi.org/10.1016/j.dsr2.2006.01.029
Goffart, A., Catalano, G., & Hecq, J. H. (2000). Factors controlling the distribution of diatoms and Phaeocystis in the Ross Sea. *Journal of Marine System*, *27*(1–3), 161–175. https://doi.org/10.1016/S0924-7963(00)00065-8
Grob, C., Ulloa, O., Claustre, H., Huot, Y., Alarcón, G., & Marie, D. (2007). Contribution of picoplankton to the total particulate organic carbon concentration in the eastern South Pacific. *Biogeosciences*, *4*(5), 837–852. https://doi.org/10.5194/bg-4-837-2007
Guidi, L., Legendre, L., Reygondeau, G., Uitz, J., Stemmann, L., & Henson, S. A. (2015). A new look at ocean carbon remineralization for estimating deepwater sequestration. *Global Biogeochemical Cycles*, *29*, 1044–1059. https://doi.org/10.1002/2014GB005063
Hasle, G. R., & Syvertsen, E. E. (1997). Chapter 2––Marine diatoms. In Tomas, C. R. (Ed.), *Identifying marine phytoplankton* (pp. 5–385). San Diego, CA: Academic Press.
Hennon, T. D., Riser, S. C., & Mecking, S. (2016). Profiling float-based observations of net respiration beneath the mixed layer. *Global Biogeochemical Cycles*, *30*, 920–932. https://doi.org/10.1002/2016GB005380
Henson, S. A., Sanders, R., & Madsen, E. (2012). Global patterns in efficiency of particulate organic carbon export and transfer to the deep ocean. *Global Biogeochemical Cycles*, *26*, GB1028. https://doi.org/10.1029/2011GB004099

Hillebrand, H., Dürselen, C.-D., Kirschtel, D., Pollingher, U., & Zohary, T. (1999). Biovolume Calculation for Pelagic and Benthic Microalgae. *Journal of Phycology*, *35*(2), 403–424. https://doi.org/10.1046/j.1529-8817.1999.3520403.x

Holm-Hansen, O., & Hewes, C. D. (2004). Deep chlorophyll-a maxima (DCMs) in Antarctic waters. I. Relationships between DCMs and the physical, chemical, and optical conditions in the upper water column. *Polar Biology*, *27*(11), 699–710. https://doi.org/10.1007/s00300-004-0641-1

Jeandel, C., Ruiz-Pino, D., Gjata, E., Poisson, A., Brunet, C., Charriaud, E. . . . Tréguer, P. (1998). KERFIX, a time-series station in the Southern Ocean: A presentation. *Journal of Marine Systems*, *17*(1–4), 555–569. https://doi.org/10.1016/S0924-7963(98)00064-5

Johnson, K., & Claustre, H. (2016). Bringing biogeochemistry into the Argo age. *Earth and Space Science News*. https://doi.org/10.1029/2016EO062427

Kopczyńska, E. E., Fiala, M., & Jeandel, C. (1998). Annual and interannual variability in phytoplankton at a permanent station off Kerguelen Islands, Southern Ocean. *Polar Biology*, *20*(5), 342–351. https://doi.org/10.1007/s003000050312

Korb, R. E., Whitehouse, M. J., Gordon, M., Ward, P., & Poulton, A. J. (2010). Summer microplankton community structure across the Scotia Sea: Implications for biological carbon export. *Biogeosciences*, *7*(1), 343–356. https://doi.org/10.5194/bg-7-343-2010

Korb, R. E., Whitehouse, M. J., Ward, P., Gordon, M., Venables, H. J., & Poulton, A. J. (2012). Regional and seasonal differences in microplankton biomass, productivity, and structure across the Scotia Sea: Implications for the export of biogenic carbon. *Deep Sea Research Part II: Topical Studies in Oceanography*, *59–60*, 67–77. https://doi.org/10.1016/j.dsr2.2011.06.006

Lasbleiz, M., Leblanc, K., Armand, L. K., Christaki, U., Georges, C., Obernosterer, I., & Quéguiner, B. (2016). Composition of diatom communities and their contribution to plankton biomass in the naturally iron-fertilized region of Kerguelen in the Southern Ocean. *FEMS Microbiology Ecology*, *92*(11), pii: fiw171. https://doi.org/10.1093/femsec/fiw171

Lasbleiz, M., Leblanc, K., Blain, S., Ras, J., Cornet-Barthaux, V., Hélias Nunige, S., & Quéguiner, B. (2014). Pigments, elemental composition (C, N, P, and Si), and stoichiometry of particulate matter in the naturally iron fertilized region of Kerguelen in the Southern Ocean. *Biogeosciences*, *11*(20), 5931–5955. https://doi.org/10.5194/bg-11-5931-2014

Laurenceau-Cornec, E. C., Trull, T. W., Davies, D. M., Bray, S. G., Doran, J., Planchon, F. . . . Blain, S. (2015). The relative importance of phytoplankton aggregates and zooplankton fecal pellets to carbon export: Insights from free-drifting sediment trap deployments in naturally iron-fertilised waters near the Kerguelen Plateau. *Biogeosciences*, *12*(4), 1007–1027. https://doi.org/10.5194/bg-12-1007-2015

Loisel, H., Bosc, E., Stramski, D., Oubelkheir, K., & Deschamps, P.-Y. (2001). Seasonal variability of the backscattering coefficient in the Mediterranean Sea based on satellite SeaWiFS imagery. *Geophysical Research Letters*, *28*(22), 4203–4206. https://doi.org/10.1029/2001GL013863

Mangoni, O., Modigh, M., Conversano, F., Carrada, G. C., & Saggiomo, V. (2004). Effects of summer ice coverage on phytoplankton assemblages in the Ross Sea, Antarctica. *Deep Sea Research Part I: Oceanographic Research Papers*, *51*(11), 1601–1617. https://doi.org/10.1016/j.dsr.2004.07.006

Manno, C., Stowasser, G., Enderlein, P., Fielding, S., & Tarling, G. A. (2015). The contribution of zooplankton faecal pellets to deep-carbon transport in the Scotia Sea (Southern Ocean). *Biogeosciences*, *12*(6), 1955–1965. https://doi.org/10.5194/bg-12-1955-2015

Marie, D., Partensky, Vaulot, F. D., & Brussaard, C. (2001). Enumeration of phytoplankton, bacteria, and viruses in marine samples, *Current Protocols in Cytometry*, *10*(11.11), 11.11.1–11.11.15.

Marra, J., Langdon, C., & Knudson, C. A. (1995). Primary production, water column changes, and the demise of a Phaeocystis bloom at the Marine Light-Mixed Layers site (59°N, 21°W) in the northeast Atlantic Ocean. *Journal of Geophysical Research*, *100*(C4), 6633–6643. https://doi.org/10.1029/94JC01127

Martin, J. H., Gordon, R. M., & Fitzwater, S. E. (1990). Iron in Antarctic waters. *Nature*, *345*(6271), 156–158. https://doi.org/10.1038/345156a0

Martz, T. R., Johnson, K. S., & Riser, S. C. (2008). Ocean metabolism observed with oxygen sensors on profiling floats in the South Pacific. *Limnology and Oceanography Methods*, *53*(5part2), 2094–2111. https://doi.org/10.4319/lo.2008.53.5_part_2.2094

Menden-Deuer, S., & Lessard, E. J. (2000). Carbon to volume relationships for dinoflagellates, diatoms, and other protist plankton. *Limnology and Oceanography*, *45*(3), 569–579. https://doi.org/10.4319/lo.2000.45.3.0569

Mikaloff Fletcher, S. E., Gruber, N., Jacobson, A. R., Doney, S. C., Dutkiewicz, S., Gerber, M. . . . Sarmiento, J. L. (2006). Inverse estimates of anthropogenic CO_2 uptake, transport, and storage by the ocean. *Global Biogeochemical Cycles*, *20*, GB2002. https://doi.org/10.1029/2005GB002530

Minas, H. J., Minas, M., & Packard, T. T. (1986). Productivity in upwelling areas deduced from hydrographic and chemical fields. *Limnology and Oceanography*, *31*(6), 1182–1206. https://doi.org/10.4319/lo.1986.31.6.1182

Moline, M. A., & Prézelin, B. B. (1996). Long-term monitoring and analyses of physical factors regulating variability in coastal Antarctic phytoplankton biomass, in situ productivity and taxonomic composition over subseasonal, seasonal and interannual time scales. *Marine Ecology Progress Series*, *145*, 143–160. https://doi.org/10.3354/meps145143

Morel, A., & Ahn, Y.-H. (1991). Optics of heterotrophic nanoflagellates and ciliates: A tentative assessment of their scattering role in oceanic waters compared to those of bacterial and algal cells. *Journal of Marine Research*, *49*(1), 177–202. https://doi.org/10.1357/002224091784968639

Nicholson, D. P., Wilson, S. T., Doney, S. C., & Karl, D. M. (2015). Quantifying subtropical North Pacific gyre mixed layer primary productivity from Seaglider observations of diel oxygen cycles. *Geophysical Research Letters*, *42*, 4032–4039. https://doi.org/10.1002/2015GL063065

Obernosterer, I., Christaki, U., Lefèvre, D., Catala, P., Van Wambeke, F., & Lebaron, P. (2008). Rapid bacterial mineralization of organic carbon produced during a phytoplankton bloom induced by natural iron fertilization in the Southern Ocean. *Deep Sea Research Part II: Topical Studies in Oceanography*, *55*(5–7), 777–789. https://doi.org/10.1016/j.dsr2.2007.12.005

Oubelkheir, K., Claustre, H., Sciandra, A., & Babin, M. (2005). Bio-optical and biogeochemical properties of different trophic regimes in oceanic waters. *Limnology and Oceanography Methods*, *50*(6), 1795–1809. https://doi.org/10.4319/lo.2005.50.6.1795

Parslow, J. S., Boyd, P. W., Rintoul, S. R., & Griffiths, F. B. (2001). A persistent subsurface chlorophyll maximum in the Interpolar Frontal Zone south of Australia: Seasonal progression and implications for phytoplankton-light-nutrient interactions. *Journal of Geophysical Research*, *106*(C12), 31543–31557. https://doi.org/10.1029/2000JC000322

Pearce, I., Davidson, A. T., Thomson, P. G., Wright, S., & van den Enden, R. (2011). Marine microbial ecology in the sub-Antarctic Zone: Rates of bacterial and phytoplankton growth and grazing by heterotrophic protists. *Deep Sea Research Part II: Topical Studies in Oceanography*, *58*(21), 2248–2259. https://doi.org/10.1016/j.dsr2.2011.05.030

Petrou, K., Kranz, S. A., Trimborn, S., Hassler, C. S., Ameijeiras, S. B., Sackett, O., . . . Davidson, A. T. (2016). Southern Ocean phytoplankton physiology in a changing climate. *J. Plant Physiology*, *203*, 135–150. https://doi.org/10.1016/j.jplph.2016.05.004

Pope, A., Wagner, P., Johnson, R., Shutler, J. D., Baeseman, J., & Newman, L. (2017). Community review of Southern Ocean satellite data needs. *Antarctic Science*, *29*(2), 97–138. https://doi.org/10.1017/S0954102016000390

Poulton, A. J., Mark Moore, C., Seeyave, S., Lucas, M. I., Fielding, S., & Ward, P. (2007). Phytoplankton community composition around the Crozet Plateau, with emphasis on diatoms and Phaeocystis. *Deep Sea Research Part II: Topical Studies in Oceanography*, *54*(18–20), 2085–2105. https://doi.org/10.1016/j.dsr2.2007.06.005

Quéroué, F., Sarthou, G., Planquette, H. F., Bucciarelli, E., Chever, F., van der Merwe, P. . . . Bowie, A. R. (2015). High variability in dissolved iron concentrations in the vicinity of the Kerguelen Islands (Southern Ocean). *Biogeosciences*, *12*(12), 3869–3883. https://doi.org/10.5194/bg-12-3869-2015

Rembauville, M., Blain, S., Armand, L., Quéguiner, B., & Salter, I. (2015). Export fluxes in a naturally iron-fertilized area of the Southern Ocean – Part 2: Importance of diatom resting spores and faecal pellets for export. *Biogeosciences*, *12*(11), 3171–3195. https://doi.org/10.5194/bg-12-3171-2015

Rembauville, M., Blain, S., Caparros, J., & Salter, I. (2016a). Particulate matter stoichiometry driven by microplankton community structure in summer in the Indian sector of the Southern Ocean. *Limnology and Oceanography Methods*, *61*(4), 1301–1321. https://doi.org/10.1002/lno.10291

Rembauville, M., Manno, C., Tarling, G. A., Blain, S., & Salter, I. (2016b). Strong contribution of diatom resting spores to deep-sea carbon transfer in naturally iron-fertilized waters downstream of South Georgia. *Deep Sea Research Part I: Oceanographic Research Papers*, *115*, 22–35. https://doi.org/10.1002/lom3.10185

Rigual-Hernández, A. S., Trull, T. W., Bray, S. G., Cortina, A., & Armand, L. K. (2015). Latitudinal and temporal distributions of diatom populations in the pelagic waters of the Subantarctic and Polar Frontal zones of the Southern Ocean and their role in the biological pump. *Biogeosciences*, *12*(18), 5309–5337. https://doi.org/10.5194/bg-12-5309-2015

Roesler, C., Uitz, J., Claustre, H., Boss, E., Xing, X., Organelli, E., . . . Barbieux, M. (2017). Recommendations for obtaining unbiased chlorophyll estimates from in situ chlorophyll fluorometers: A global analysis of WET Labs ECO sensors. *Limnology and Oceanography Methods*, *15*, 572–585. https://doi.org/10.1002/lom3.10185

Rontani, J.-F., Beker, B., Raphel, D., & Baillet, G. (1995). Photodegradation of chlorophyll phytyl chain in dead phytoplanktonic cells. *Journal of Photochemistry and Photobiology A: Chemistry*, *85*(1), 137–142. https://doi.org/10.1016/1010-6030(94)03891-W

Sabine, C. L., Feely, R. A., Gruber, N., Key, R. M., Lee, K., Bullister, J. L. . . . Rios, (2004). The Oceanic Sink for Anthropogenic CO_2. *Science*, *305*(5682), 367–371. https://doi.org/10.1126/science.1097403

Salter, I., Kemp, A. E. S., Moore, C. M., Lampitt, R. S., Wolff, G. A., & Holtvoeth, J. (2012). Diatom resting spore ecology drives enhanced carbon export from a naturally iron-fertilized bloom in the Southern Ocean. *Global Biogeochemical Cycles*, *26*, GB1014. https://doi.org/10.1029/2010GB003977

Sauzède, R., Claustre, H., Pasqueron de Fommervault, O., Bittig, H., Gattuso, J.-P., Legendre, L., & Johnson, K. S. (2017). Estimates of water-column nutrients and carbonate system parameters in the global ocean: A novel approach based on neural networks. *Frontiers in Marine Science*, *4*, 128. https://doi.org/10.3389/fmars.2017.00128

Schmechtig, C., Poteau, A., Claustre, H., D'ortenzio, F., Dall'olmo, G., & Boss, E. (2015). Processing Bio-Argo particle backscattering at the DAC level. *Argo Data Management*, https://doi.org/10.13155/39459

Simon, M., Cho, B. C., & Azam, F. (1992). Significance of bacterial biomass in lakes and the ocean: Comparison to phytoplankton biomass and biogeochemical implications. *Marine Ecology Progress Series*, *86*, 103–111. https://doi.org/10.3354/meps086103

Smayda, T. J. (1969). Some measurements of the sinking rate of fecal pellets. *Limnol.ogy and Oceanography*, *14*(4), 621–625. https://doi.org/10.4319/lo.1969.14.4.0621

Stramski, D., & Kiefer, D. A. (1991). Light scattering by microorganisms in the open ocean. *Progress in Oceanography*, *28*(4), 343–383. https://doi.org/10.1016/0079-6611(91)90032-H

Stramski, D., Reynolds, R. A., Babin, M., Kaczmarek, S., Lewis, M. R., Röttgers, R., . . . Claustre, H. (2008). Relationships between the surface concentration of particulate organic carbon and optical properties in the eastern South Pacific and eastern Atlantic Oceans. *Biogeosciences*, *5*(1), 171–201. https://doi.org/10.5194/bg-5-171-2008

Stramski, D., Reynolds, R. A., Kahru, M., & Mitchell, B. G. (1999). Estimation of particulate organic carbon in the ocean from satellite remote sensing. *Science*, *285*(5425), 239–242.

Swart, S., Speich, S., Ansorge, I. J., & Lutjeharms, J. R. E. (2010). An altimetry-based gravest empirical mode south of Africa: 1. Development and validation. *Journal of Geophysical Research*, *115*, C03002. https://doi.org/10.1029/2009JC005299

Thomalla, S. J., Fauchereau, N., Swart, S., & Monteiro, P. M. S. (2011). Regional scale characteristics of the seasonal cycle of chlorophyll in the Southern Ocean. *Biogeosciences*, *8*(10), 2849–2866. https://doi.org/10.5194/bg-8-2849-2011

Thomalla, S. J., Racault, M.-F., Swart, S., & Monteiro, P. M. S. (2015). High-resolution view of the spring bloom initiation and net community production in the Subantarctic Southern Ocean using glider data. *ICES Journal of Marine Sciences*, *72*(6), 1999–2020. https://doi.org/10.1093/icesjms/fsv105

Thornton, D. C. O. (2002). Diatom aggregation in the sea: Mechanisms and ecological implications. *European Journal of Phycology*, *37*(2), 149–161. https://doi.org/10.1017/S0967026202003657

Uitz, J., Claustre, H., Griffiths, F. B., Ras, J., Garcia, N., & Sandroni, V. (2009). A phytoplankton class-specific primary production model applied to the Kerguelen Islands region (Southern Ocean). *Deep Sea Research Part I: Oceanographic Research Papers*, *56*(4), 541–560. https://doi.org/10.1016/j.dsr.2008.11.006

Vaillancourt, R. D., Brown, C. W., Guillard, R. R. L., & Balch, W. M. (2004). Light backscattering properties of marine phytoplankton: Relationships to cell size, chemical composition and taxonomy. *Journal of Plankton Research*, *26*(2), 191–212. https://doi.org/10.1093/plankt/fbh012

Verity, P. G., Robertson, C. Y., Tronzo, C. R., Andrews, M. G., Nelson, J. R., & Sieracki, M. E. (1992). Relationships between cell volume and the carbon and nitrogen content of marine photosynthetic nanoplankton. *Limnology and Oceanography*, *37*(7), 1434–1446. https://doi.org/10.4319/lo.1992.37.7.1434

Volten, H., de Haan, J. F., Hovenier, J. W., Schreurs, R., Vassen, W., Dekker, A. G., . . . Wouts, R. (1998). Laboratory measurements of angular distributions of light scattered by phytoplankton and silt. *Limnology and Oceanography*, *43*(6), 1180–1197. https://doi.org/10.4319/lo.1998.43.6.1180

Whitmire, A. L., Pegau, W. S., Karp-Boss, L., Boss, E., & Cowles, T. J. (2010). Spectral backscattering properties of marine phytoplankton cultures. *Optics Express*, *18*(14), 15073. https://doi.org/10.1364/OE.18.015073

Xing, X., Claustre, H., Blain, S., D'ortenzio, F., Antoine, D., Ras, J., & Guinet, C. (2012). Quenching correction for in vivo chlorophyll fluorescence acquired by autonomous platforms: A case study with instrumented elephant seals in the Kerguelen region (Southern Ocean). *Limnology and Oceanography Methods*, *10*, 483–495. https://doi.org/10.4319/lom.2012.10.483

Xing, X., Morel, A., Claustre, H., Antoine, D., D'ortenzio, F., Poteau, A., & Mignot, A. (2011). Combined processing and mutual interpretation of radiometry and fluorimetry from autonomous profiling Bio-Argo floats: Chlorophyll a retrieval. *Journal of Geophysical Research*, *116*, C06020. https://doi.org/10.1029/2010JC006899